

Dislocation Etching Solutions for Mercury Cadmium Selenide

by Kevin Doyle and Sudhir Trivedi

ARL-CR-0744

September 2014

prepared by

**Oak Ridge Associated Universities
4692 Millennium Drive, Suite 101
Belcamp MD 21017**

under contract

W811NF-12-2-0019

NOTICES

Disclaimers

The findings in this report are not to be construed as an official Department of the Army position unless so designated by other authorized documents.

Citation of manufacturer's or trade names does not constitute an official endorsement or approval of the use thereof.

Destroy this report when it is no longer needed. Do not return it to the originator.

Army Research Laboratory

Adelphi, MD 20783-1138

ARL-CR-0744

September 2014

Dislocation Etching Solutions for Mercury Cadmium Selenide

Kevin Doyle and Sudhir Trivedi
Sensors and Electron Devices Directorate, ARL

prepared by

Oak Ridge Associated Universities
4692 Millennium Drive, Suite 101
Belcamp MD 21017

under contract

W811NF-12-2-0019

REPORT DOCUMENTATION PAGE			Form Approved OMB No. 0704-0188		
<p>Public reporting burden for this collection of information is estimated to average 1 hour per response, including the time for reviewing instructions, searching existing data sources, gathering and maintaining the data needed, and completing and reviewing the collection information. Send comments regarding this burden estimate or any other aspect of this collection of information, including suggestions for reducing the burden, to Department of Defense, Washington Headquarters Services, Directorate for Information Operations and Reports (0704-0188), 1215 Jefferson Davis Highway, Suite 1204, Arlington, VA 22202-4302. Respondents should be aware that notwithstanding any other provision of law, no person shall be subject to any penalty for failing to comply with a collection of information if it does not display a currently valid OMB control number.</p> <p>PLEASE DO NOT RETURN YOUR FORM TO THE ABOVE ADDRESS.</p>					
1. REPORT DATE (DD-MM-YYYY) September 2014		2. REPORT TYPE Final		3. DATES COVERED (From - To) 06/2014	
4. TITLE AND SUBTITLE Dislocation Etching Solutions for Mercury Cadmium Selenide		5a. CONTRACT NUMBER W811NF-12-2-0019			
		5b. GRANT NUMBER			
		5c. PROGRAM ELEMENT NUMBER			
6. AUTHOR(S) Kevin Doyle and Sudhir Trivedi		5d. PROJECT NUMBER W811NF-12-2-0019			
		5e. TASK NUMBER			
		5f. WORK UNIT NUMBER			
7. PERFORMING ORGANIZATION NAME(S) AND ADDRESS(ES) Oak Ridge Associated Universities 4692 Millennium Drive, Suite 101 Belcamp MD 21017		8. PERFORMING ORGANIZATION REPORT NUMBER ARL-CR-0744			
9. SPONSORING/MONITORING AGENCY NAME(S) AND ADDRESS(ES) US Army Research Laboratory ATTN: RDRL-SEE-I 2800 Powder Mill Road Adelphi, MD 20783-1138		10. SPONSOR/MONITOR'S ACRONYM(S)			
		11. SPONSOR/MONITOR'S REPORT NUMBER(S)			
12. DISTRIBUTION/AVAILABILITY STATEMENT Approved for public release; distribution unlimited.					
13. SUPPLEMENTARY NOTES					
14. ABSTRACT <p>Mercury cadmium selenide ($Hg_{1-x}Cd_xSe$) is a possible alternative material to mercury cadmium telluride ($Hg_{1-x}Cd_xTe$) for infrared (IR) sensor applications, but etch pit density (EPD) measurements are required to measure dislocations that affect device performance. No EPD solutions have been reported for $Hg_{1-x}Cd_xSe$, and standard EPD solutions for $Hg_{1-x}Cd_xTe$ have proved ineffective. Thus, a new etching solution is required for EPD measurements of $Hg_{1-x}Cd_xSe$. Samples were etched in various solutions and the resulting pits were observed using Nomarski microscopy and scanning electron microscopy (SEM). Solutions consisting of nitric and hydrochloric acid produced mainly trapezoid-shaped pits, but with flat or rounded bottoms rather than converging to a single point as expected. One solution consisting of nitric, hydrochloric, and phosphoric acid produced hexagonal pits that converged at a single point as expected, but this solution was unstable and these pits could not be repeated on any other sample. Further experiments are required to produce an etching solution that consistently forms pits that converge on a single point and then transmission electron microscopy (TEM) measurements will need to be performed to confirmed that these pits correspond to a dislocation—thus enabling EPD measurement of $Hg_{1-x}Cd_xSe$.</p>					
15. SUBJECT TERMS Mercury cadmium selenide, etch pits, dislocations, preferential etching solutions					
16. SECURITY CLASSIFICATION OF:			17. LIMITATION OF ABSTRACT UU	18. NUMBER OF PAGES 24	19a. NAME OF RESPONSIBLE PERSON Kevin Doyle
a. REPORT Unclassified	b. ABSTRACT Unclassified	c. THIS PAGE Unclassified			19b. TELEPHONE NUMBER (Include area code) (301) 394-3390

Contents

List of Figures	iv
Acknowledgments	v
1. Introduction	1
2. Etch Solutions	1
2.1 Nitric and Hydrochloric Acid.....	1
2.2 Nitric Acid, Hydrochloric Acid, and Complexing Agents.....	5
2.3 Nitric, Hydrochloric, and Phosphoric Acid.....	7
2.4 Polisar Etch.....	9
3. Etch Pit Summary	10
4. Etching of ZnTe Buffer Layer	10
5. Further Work	11
6. References	13
List of Symbols, Abbreviations, and Acronyms	14
Distribution List	15

List of Figures

Fig. 1	Hg _{0.84} Cd _{0.16} Se sample SZ48-E2 viewed under Nomarski 100×, a) unetched and b) etched 20 s in HNO ₃ :HCl (2:1), then 20 s 50% H ₂ SO ₄	2
Fig. 2	Hg _{0.84} Cd _{0.16} Se sample SZ48-E3 a) unetched, and etched 20 s in HNO ₃ :HCl (5:4) viewed under, b) Nomarski 100×, c) SEM 4×,485, and d) SEM 25×,374	3
Fig. 3	Pieces of Hg _{0.79} Cd _{0.21} Se sample SZ56 viewed under Nomarski 100× after etching in HNO ₃ :HCl (2:1) for a) 5, b) 10, c) 15, and d) 20 s. The red lines were a measure of pit size.	4
Fig. 4	Pit size (top) and etch depth (bottom) vs. etch time for pieces of SZ56 etched in HNO ₃ :HCl (2:1)	4
Fig. 5	Hg _{0.81} Cd _{0.19} Se sample SZ50-GR1 viewed under Nomarski 100× a) pre-etch and b) etched 5 s in HNO ₃ :HCl:H ₂ O (2:1:3).....	5
Fig. 6	Hg _{0.82} Cd _{0.18} Se sample SZ45-E5 under Nomarski 100× a) pre-etch and b) etched 10 s in HNO ₃ :HCl:HF (4:2:1).....	5
Fig. 7	Hg _{0.81} Cd _{0.19} Se sample SZ50-GR12 a) pre-etched, Nomarski 100× and then etched 40 s in HNO ₃ :HCl:CH ₃ COOH (2:1:1) viewed under, b) Nomarski 100×, c) SEM 6,246×, and d) SEM 64,802×	6
Fig. 8	Hg _{0.81} Cd _{0.19} Se sample SZ50-GR17 etched 20 s in HNO ₃ :HCl:C ₃ H ₆ O ₃ (2:1:2) viewed under a) SEM 39,749× and b) SEM, 51,548×	7
Fig. 9	Hg _{0.71} Cd _{0.29} Se sample SZ40-E3 etched 20 s in HNO ₃ :HCl:H ₃ PO ₄ (20:10:5) viewed under a) Nomarski 20×, b) Nomarski 100×, c) SEM 2,554 ×, d) SEM 13,526×, e) SEM 9,572×, and f) SEM 16,098×	8
Fig. 10	Sample SZ6 viewed under Nomarski 100× a) unetched, b) etched in Polisar for 1 min, c) etched in Polisar for 2 min, and d) etched in Polisar for 2 min then Br ₂ -methanol for 2 s	9
Fig. 11	Piece of ZT072406N viewed under Nomarski 20× a) unetched, and etched HNO ₃ :HCl:C ₃ H ₆ O ₃ (2:1:2), b) 5 s, c) 10 s (center), and d) 10 s (near edge).....	11

Acknowledgments

We would also like to thank Dr J David Benson at the Night Vision and Electronic Sensors Directorate for his input on the process. Research was sponsored by the US Army Research Laboratory and was accomplished under Cooperative Agreement # W911NF-12-2-0019.

INTENTIONALLY LEFT BLANK.

1. Introduction

Mercury cadmium selenide ($\text{Hg}_{1-x}\text{Cd}_x\text{Se}$) is a possible alternative material to mercury cadmium telluride ($\text{Hg}_{1-x}\text{Cd}_x\text{Te}$) for infrared (IR) sensor applications. The bandgap of $\text{Hg}_{1-x}\text{Cd}_x\text{Se}$ can be tuned across the same spectral regions as $\text{Hg}_{1-x}\text{Cd}_x\text{Te}$, and $\text{Hg}_{1-x}\text{Cd}_x\text{Se}$ is also closely lattice-matched to gallium antimonide (GaSb). Since GaSb is available as a large-area substrate, $\text{Hg}_{1-x}\text{Cd}_x\text{Se}$ epitaxial layers can potentially be grown on GaSb substrates with fewer misfit dislocations, which have been shown to be detrimental to long wave infrared $\text{Hg}_{1-x}\text{Cd}_x\text{Te}$ devices.¹

In order to verify this, a reliable technique for measuring dislocations needs to be established for $\text{Hg}_{1-x}\text{Cd}_x\text{Se}$. For samples where the dislocation densities are too low ($<10^8 \text{ cm}^{-2}$) to measure with tunneling electron microscopy (TEM), this is typically done with etch pit density (EPD) measurements. EPD measurements are performed by placing samples in a solution that etches slowly for the polarity and main orientation of the sample, but etches at a faster rate for other crystallographic orientations. As a result, the etch produces a pit where dislocations intersect the crystallographic surface, so the density of dislocations can be measured from the density of pits observed after etching.

The morphology and size of etch pits will vary depending on the etch solution and the crystallography of the material, but in general the etch pits will form geometric shapes that emanate from a single point where the dislocation is located.² No EPD solutions have been reported for $\text{Hg}_{1-x}\text{Cd}_x\text{Se}$, and standard EPD solutions for $\text{Hg}_{1-x}\text{Cd}_x\text{Te}$ and cadmium zinc telluride, such as the Benson etch³ and the Everson etch,⁴ proved ineffective. In order to establish an EPD solution for $\text{Hg}_{1-x}\text{Cd}_x\text{Se}$, $\text{Hg}_{1-x}\text{Cd}_x\text{Se}$ samples were etched in various solutions and the resulting pits were observed using Nomarski microscopy and scanning electron microscopy (SEM). The samples were grown via molecular beam epitaxy on silicon substrates with zinc telluride buffer layers (ZnTe/Si).⁵

2. Etch Solutions

2.1 Nitric and Hydrochloric Acid

Previously, solutions consisting of nitric acid (HNO_3) and hydrochloric acid (HCl) had been shown to produce etch pits on mercury selenide (HgSe) and cadmium selenide (CdSe),⁶ and so solutions consisting of these two acids were tested. It was expected that the pits would be triangular, which is typical for the Benson etch on $\text{Hg}_{1-x}\text{Cd}_x\text{Te}$. However, a solution of $\text{HNO}_3\text{:HCl}$ (2:1) produced trapezoid-shaped pits, as seen in Fig. 1. Previous reports suggested that these etchants could leave an Se-film on the surface, so initially the samples were etched

briefly dilute sulfuric acid (50% H_2SO_4) to remove any remaining films. The pits had the same shape and orientation, which is expected for a dislocation etch pit, but they appeared to have curved bottoms rather than the expected faceted walls emanating from a single point.

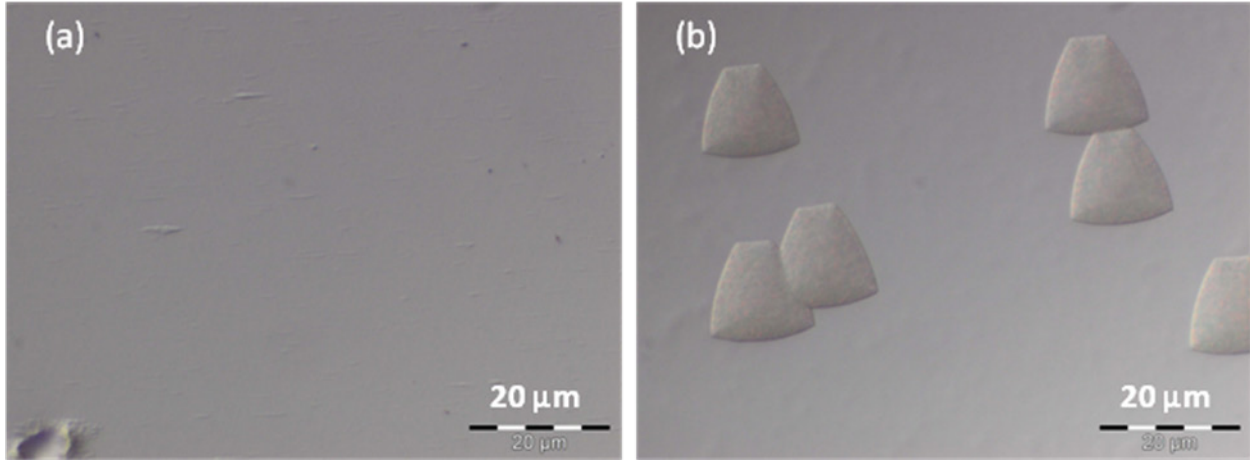


Fig. 1 $\text{Hg}_{0.84}\text{Cd}_{0.16}\text{Se}$ sample SZ48-E2 viewed under Nomarski 100 \times , a) unetched and b) etched 20 s in $\text{HNO}_3\text{:HCl}$ (2:1), then 20 s 50% H_2SO_4

At first, the $\text{HNO}_3\text{:HCl}$ ratio and etch time were varied to control the etching speed and formation of the pits. However, changing the ratio started changing the shape of the pit, making the shape less defined, as seen in Fig. 2. Based on this, it was decided that the (2:1) $\text{HNO}_3\text{:HCl}$ ratio was preferred. An estimate for the etch rate for this solution was determined by etching pieces of an $\text{Hg}_{0.79}\text{Cd}_{0.21}\text{Se}$ sample SZ52 for different etch times, and then using a Tencor step profilometer to determine the change in sample height. The base-to-height length of the trapezoidal pits was also estimated from Nomarski 100 \times images, as shown in Fig. 3.

Based on these rough measurements, given in Fig. 4, it appears that $\text{HNO}_3\text{:HCl}$ (2:1) etched at a rate of roughly 0.14 $\mu\text{m/s}$. Measurements from sample SZ56-GR5 (the sample etched for 25 s) are probably not trustworthy as at that point as the etch had been heavily used on the previous samples, so the etch was remixed for the 30-s etch. Not counting SZ56-GR5, the pit size appeared to increase at a rate of 0.82 $\mu\text{m/s}$ for 20 s, then it leveled off at around 16 μm .

In order to control the etch rate, it was decided to keep the $\text{HNO}_3\text{:HCl}$ ratio at (2:1) and add complexing agents to slow down the etch process.

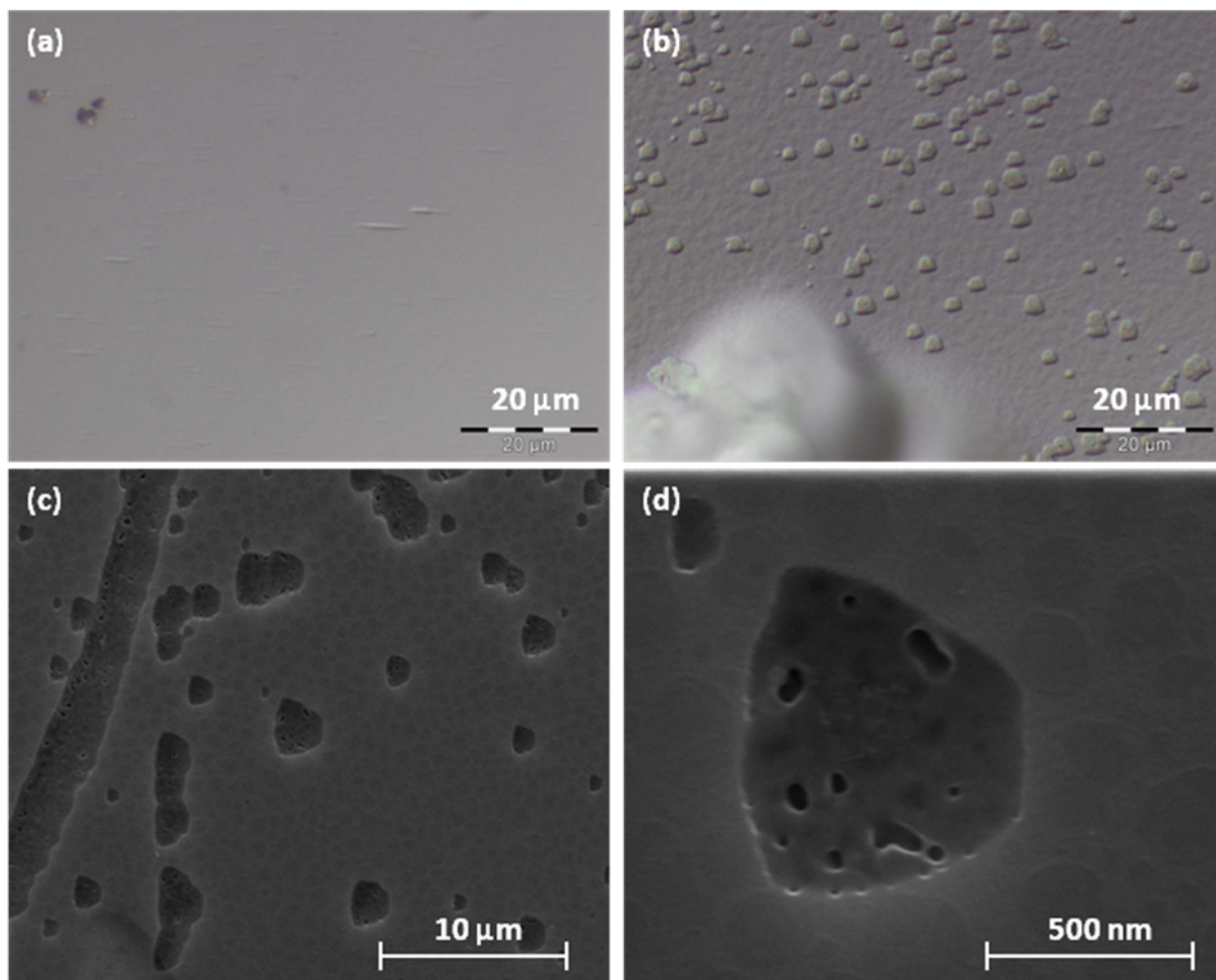


Fig. 2 $\text{Hg}_{0.84}\text{Cd}_{0.16}\text{Se}$ sample SZ48-E3 a) unetched, and etched 20 s in $\text{HNO}_3\text{:HCl}$ (5:4) viewed under, b) Nomarski 100 \times , c) SEM 4 \times ,485, and d) SEM 25 \times ,374

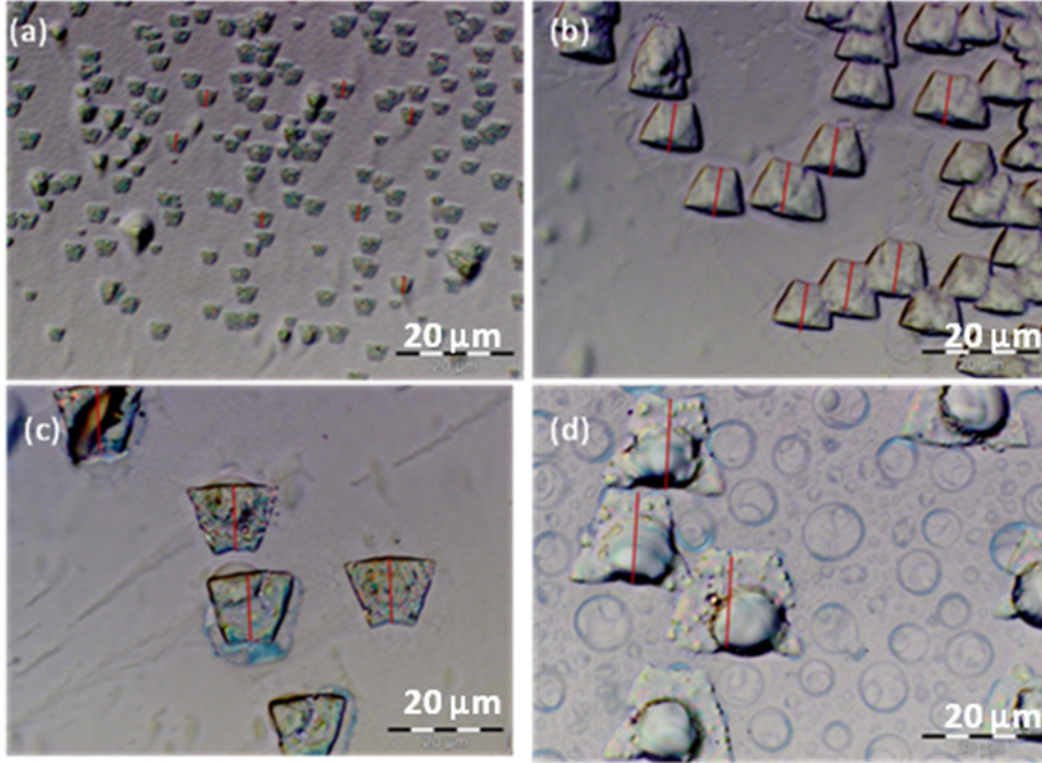


Fig. 3 Pieces of $\text{Hg}_{0.79}\text{Cd}_{0.21}\text{Se}$ sample SZ56 viewed under Nomarski 100 \times after etching in $\text{HNO}_3\text{:HCl}$ (2:1) for a) 5, b) 10, c) 15, and d) 20 s. The red lines were a measure of pit size.

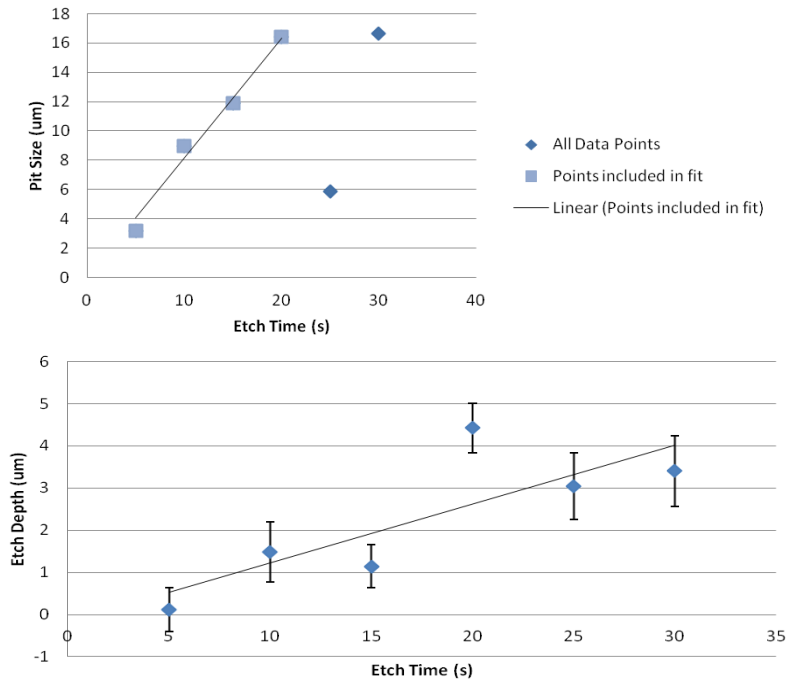


Fig. 4 Pit size (top) and etch depth (bottom) vs. etch time for pieces of SZ56 etched in $\text{HNO}_3\text{:HCl}$ (2:1)

2.2 Nitric Acid, Hydrochloric Acid, and Complexing Agents

Complexing agents were then added to the $\text{HNO}_3\text{:HCl}$ (2:1) solution. These include de-ionized water (H_2O), hydrofluoric acid (HF), lactic acid ($\text{C}_3\text{H}_6\text{O}_3$), acetic acid (CH_3COOH), and phosphoric acid (H_3PO_4). Solutions with H_2O produced some discoloration, as seen in Fig. 5, which at first was thought to be an oxidation effect, but could also be the etch solution reaching the ZnTe layer as discussed in section 4. A solution of $\text{HNO}_3\text{:HCl:HF}$ (4:2:1) only appeared to roughen the surface (Fig. 6), so H_2O and HF were dropped as complexing agents.

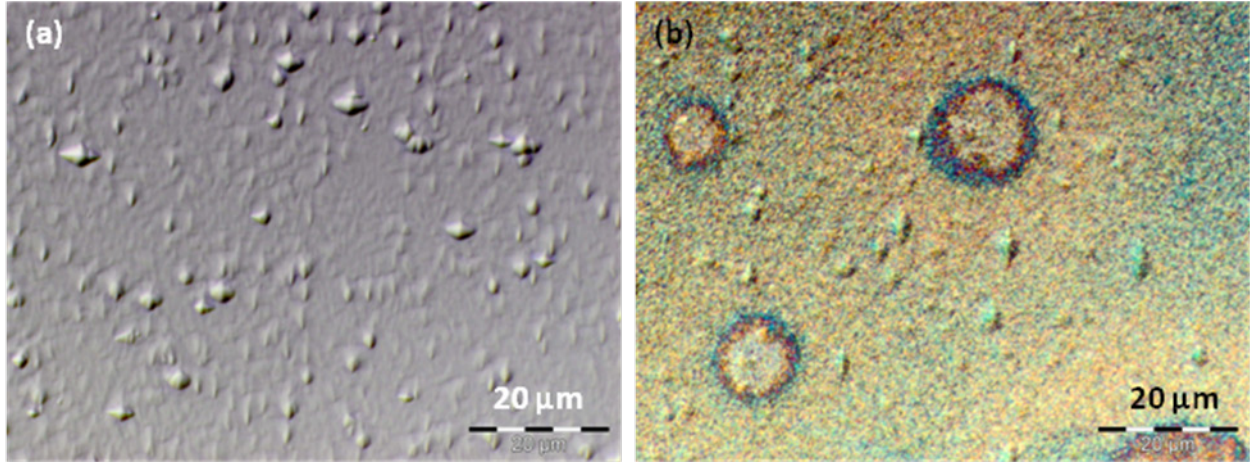


Fig. 5 $\text{Hg}_{0.81}\text{Cd}_{0.19}\text{Se}$ sample SZ50-GR1 viewed under Nomarski 100 \times a) pre-etch and b) etched 5 s in $\text{HNO}_3\text{:HCl:H}_2\text{O}$ (2:1:3)

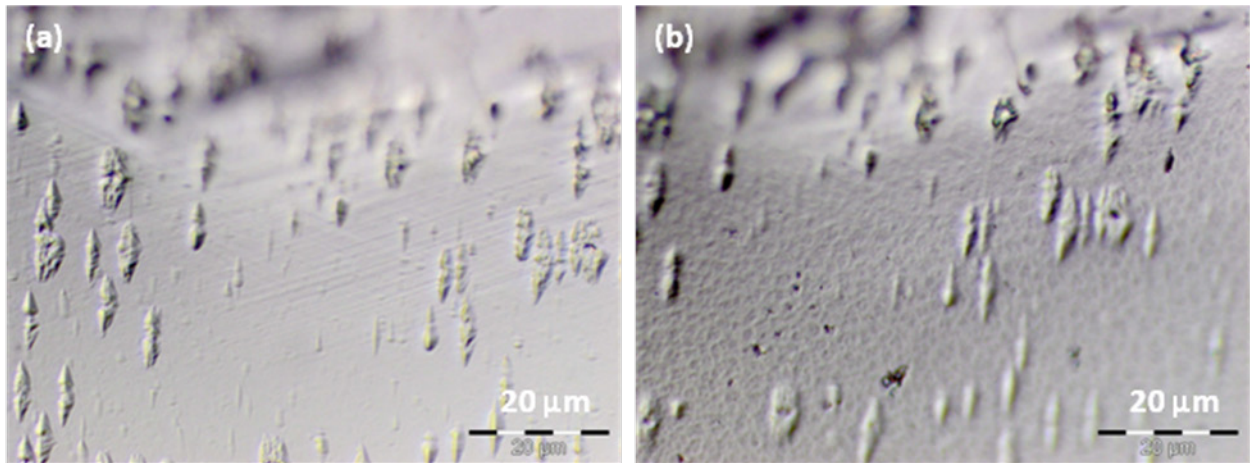


Fig. 6 $\text{Hg}_{0.82}\text{Cd}_{0.18}\text{Se}$ sample SZ45-E5 under Nomarski 100 \times a) pre-etch and b) etched 10 s in $\text{HNO}_3\text{:HCl:HF}$ (4:2:1)

Samples etched with an acetic acid and lactic acid produced the trapezoidal pits, but with the same curved bottoms and pits-within-pits observed before, as shown in Fig. 7. Some samples etched in solutions with lactic acid appeared to produce pits with well-defined walls, as seen in Fig. 8, which is to be expected for a pit corresponding to a dislocation. However, these pits still had flat bottoms, rather than converging on a single point, as should be the case.

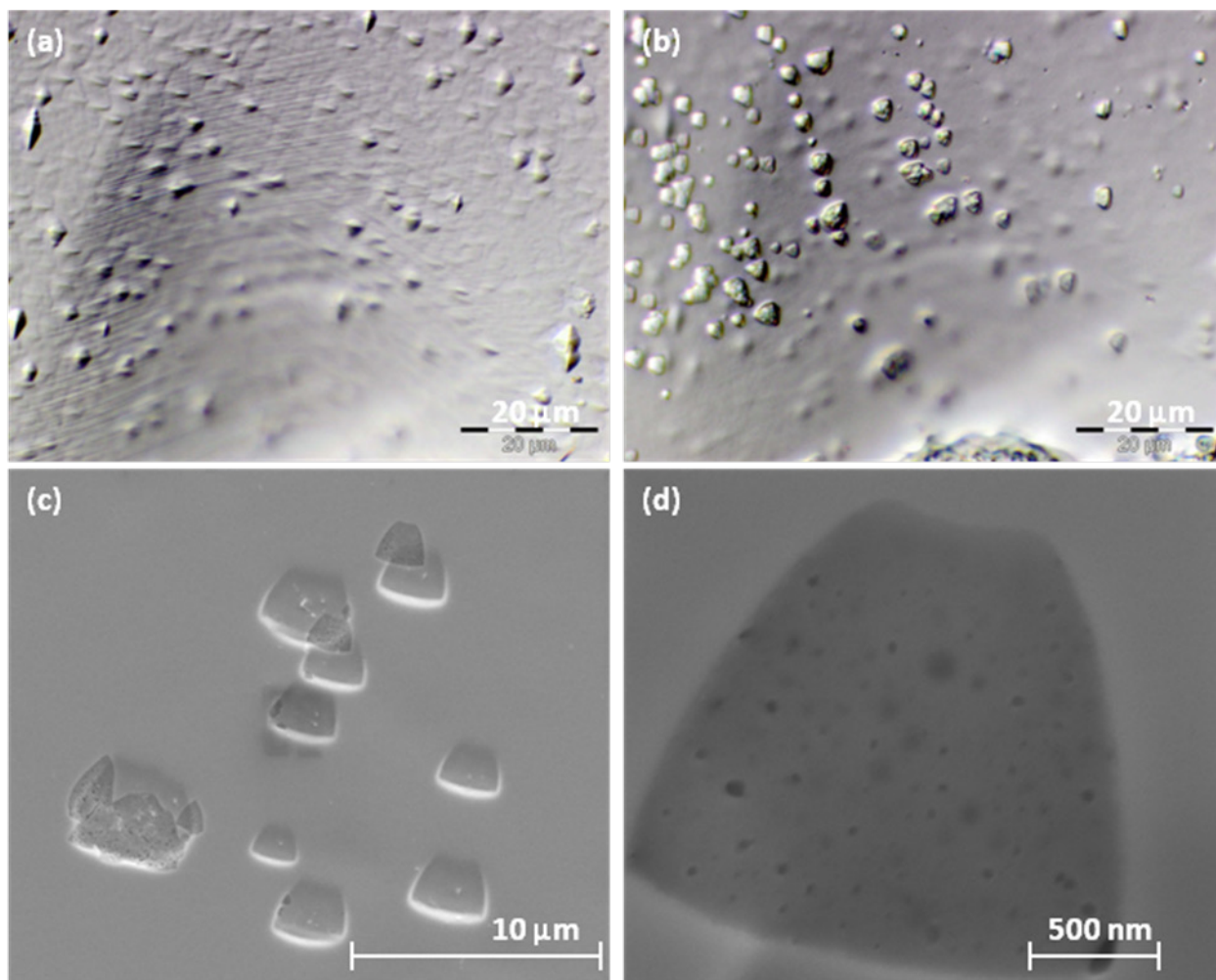


Fig. 7 $\text{Hg}_{0.81}\text{Cd}_{0.19}\text{Se}$ sample SZ50-GR12 a) pre-etched, Nomarski 100 \times and then etched 40 s in $\text{HNO}_3\text{:HCl:CH}_3\text{COOH}$ (2:1:1) viewed under, b) Nomarski 100 \times , c) SEM 6,246 \times , and d) SEM 64,802 \times

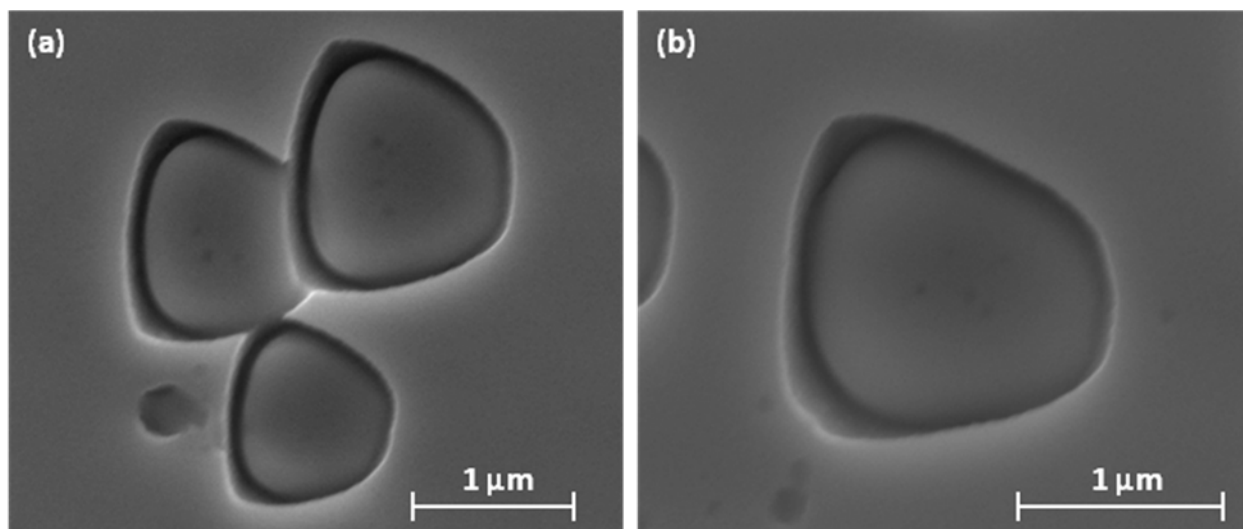


Fig. 8 $\text{Hg}_{0.81}\text{Cd}_{0.19}\text{Se}$ sample SZ50-GR17 etched 20 s in $\text{HNO}_3:\text{HCl}:\text{C}_3\text{H}_6\text{O}_3$ (2:1:2) viewed under a) SEM 39,749 \times and b) SEM, 51,548 \times

2.3 Nitric, Hydrochloric, and Phosphoric Acid

Samples etched in solutions containing H_3PO_4 mostly produced trapezoidal pits, but the exact shape of the pits was inconsistent from sample to sample or even across the surfaces of the same sample. The color of the etch solutions was observed to change rapidly, and the etching rate quickly deteriorated once the solution was made, making these etching results very inconsistent.

However, one section of $\text{Hg}_{0.71}\text{Cd}_{0.29}\text{Se}$ sample SZ40-E3 etched 20 s in $\text{HNO}_3:\text{HCl}:\text{H}_3\text{PO}_4$ (20:10:5) produced pits that were hexagonal, rather than trapezoidal, as seen in Fig. 9.

Furthermore, while some of these pits appeared to be filled with debris, *the clear pits appeared to converge on a single point with faceted walls, which is what is expected for pits emanating from a dislocation*. Moreover, Figs. 9a and 9b shows pits along slip lines, indicative of revealing the dislocations. These hexagonal pits were the most likely to represent dislocations, but due to the volatility of the etch solution these pits could not be reproduced on any other samples.

Additionally, while many of the hexagonal pits are clear, others appear to be filled with debris. This could be from material being redeposited back into the etch pits rather than being removed in the etch process. By extension, this redeposition back into the pits could be the reason the trapezoidal pits appear to have curved uneven bottoms rather than the expected single-point bottoms that would indicate a dislocation.

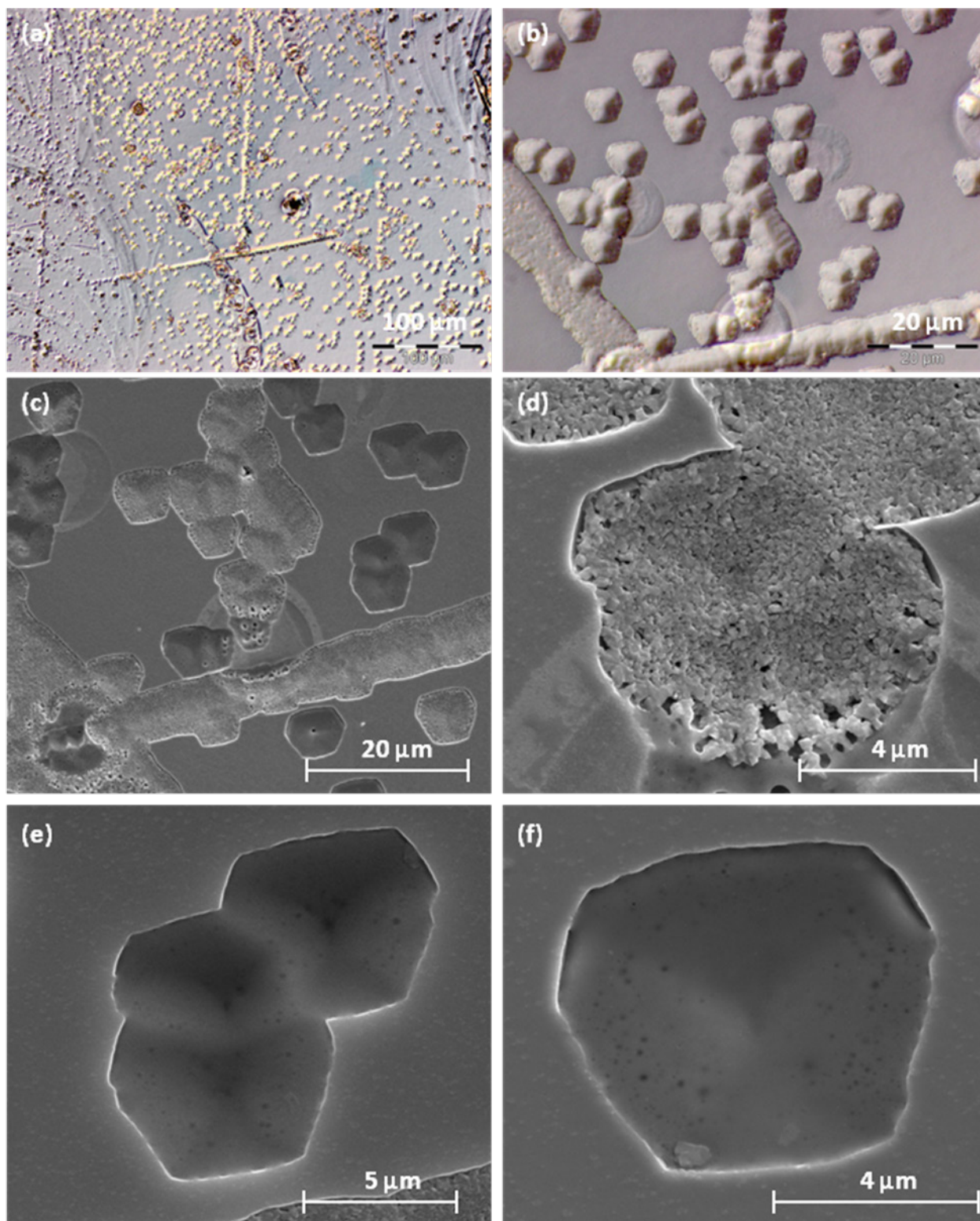


Fig. 9 $\text{Hg}_{0.71}\text{Cd}_{0.29}\text{Se}$ sample SZ40-E3 etched 20 s in $\text{HNO}_3:\text{HCl}:\text{H}_3\text{PO}_4$ (20:10:5) viewed under a) Nomarski 20 \times , b) Nomarski 100 \times , c) SEM 2,554 \times , d) SEM 13,526 \times , e) SEM 9,572 \times , and f) SEM 16,098 \times

2.4 Polisar Etch

Prior to any of the etch work discussed above, one attempt was made to use the Polisar etch on $\text{Hg}_{1-x}\text{Cd}_x\text{Se}$. A previously reported etching study of bulk-grown $\text{Hg}_{1-x}\text{Zn}_x\text{Se}$ wafers cleaved along the [111] surface gave EPD measurements after soaking in an ambient solution of 90:60:25:5 H_2O , HNO_3 , HCl , and 0.1 cc bromine (Br_2) in acetic acid. This etch produced a Se film, which was removed by placing the samples in a Br_2 -methanol solution for 1–2 s.⁷

A couple $\text{Hg}_{1-x}\text{Cd}_x\text{Se}$ samples were etched in this solution, which produced some small pits after ~2 min, as seen in Fig. 10. At the time, we thought the pits looked too circular, but perhaps they were not given time to form.

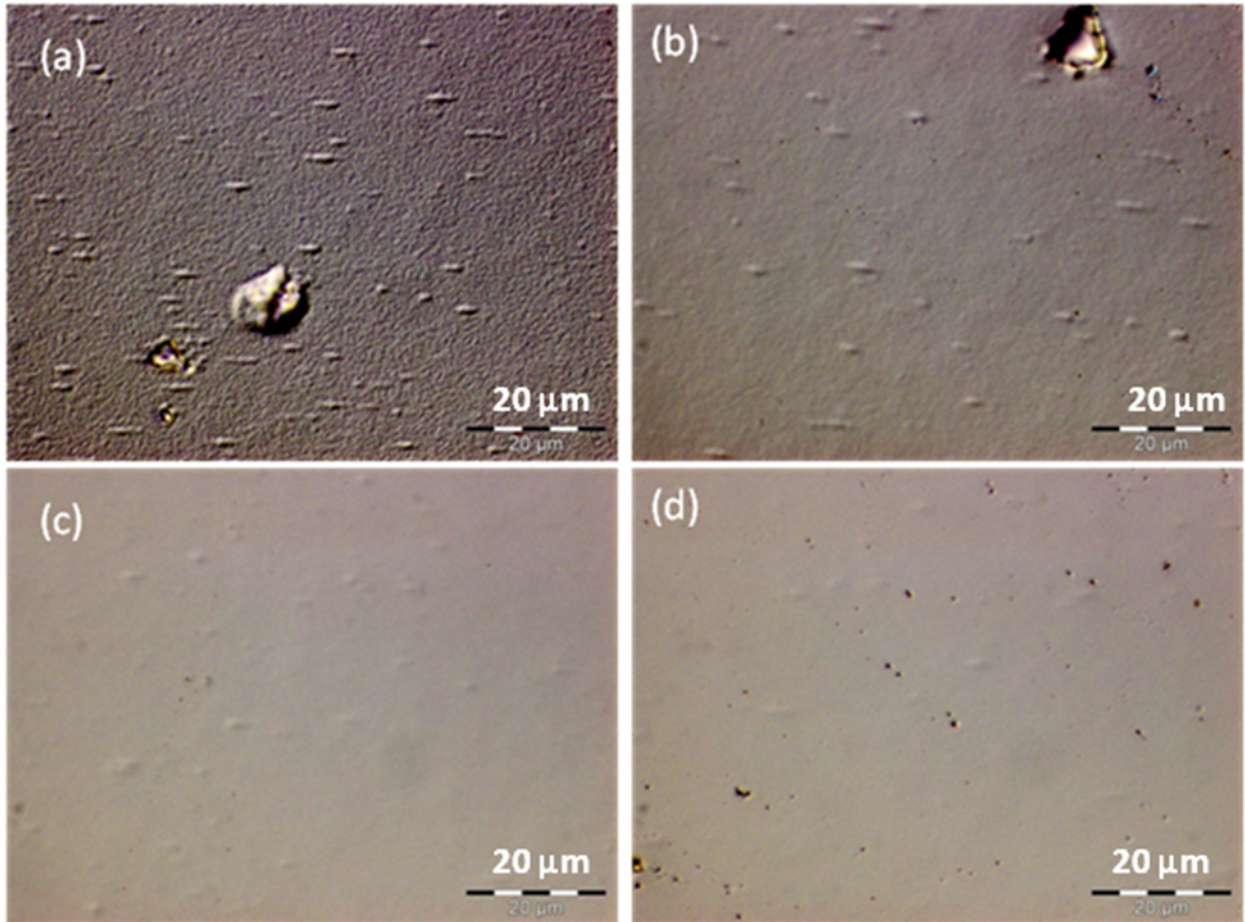


Fig. 10 Sample SZ6 viewed under Nomarski 100× a) unetched, b) etched in Polisar for 1 min, c) etched in Polisar for 2 min, and d) etched in Polisar for 2 min then Br_2 -methanol for 2 s

3. Etch Pit Summary

Though the distinctness of the etch pits varied with the etch solution, many different solutions produced recognizably trapezoidal pits. These pits likely correspond to dislocations for the following reasons:

1. **Shape is consistent:** Pits are consistently trapezoidal, except for the one case where they were hexagonal.
2. **Orientation is consistent:** The trapezoids are always orientated perpendicular to the [211] wafer flat, suggesting they are sensitive to the crystallography.
3. **Slip lines:** As we went on, we began inducing slip lines by indenting the samples with a pin prior to etching. The pits would form along the lines of stress (the ones we created and other ones we didn't), which was expected as dislocations also form along stress lines.

However, the trapezoidal pits do have some features that are inconsistent with dislocation pits:

1. **Walls are not faceted:** A dislocation pit should have clearly faceted walls that correspond to the crystallographic faces, while the trapezoidal pits are often curved.
2. **The pits do not converge to single point:** The bottom of a dislocation pit should be at a single point corresponding to the dislocation. Most of the trapezoidal pits have curved or flat bottoms.

The hexagonal pits did have faceted walls and single-point bottoms, and some of these pits also appear to have debris leftover from etching. Thus it's possible that one reason for the odd shape of the trapezoidal pits is that material is being redeposited in the pit during etching, covering up the faceted walls and producing the curved/flat bottoms instead. Further tests (possibly TEM) should be performed to confirm this.

4. Etching of ZnTe Buffer Layer

Greater control over the etch rate is needed because of the effect these etchants appear to have on the ZnTe buffer layer. After etching, some areas of the samples appeared to suddenly develop very rough and discolored surfaces. This was attributed to the fact that the acid-based etchants have a strong effect on ZnTe. A ZnTe/Si sample, ZT072406N, was etched for 5 s, then an additional 5 s in a $\text{HNO}_3\text{:HCl:C}_3\text{H}_6\text{O}_3$ (2:1:2) solution. After 5 s, the surface became very rough, and after 10 s, the layer was actually dissolving leaving the Si substrate behind near the edges, as seen in Fig. 11.

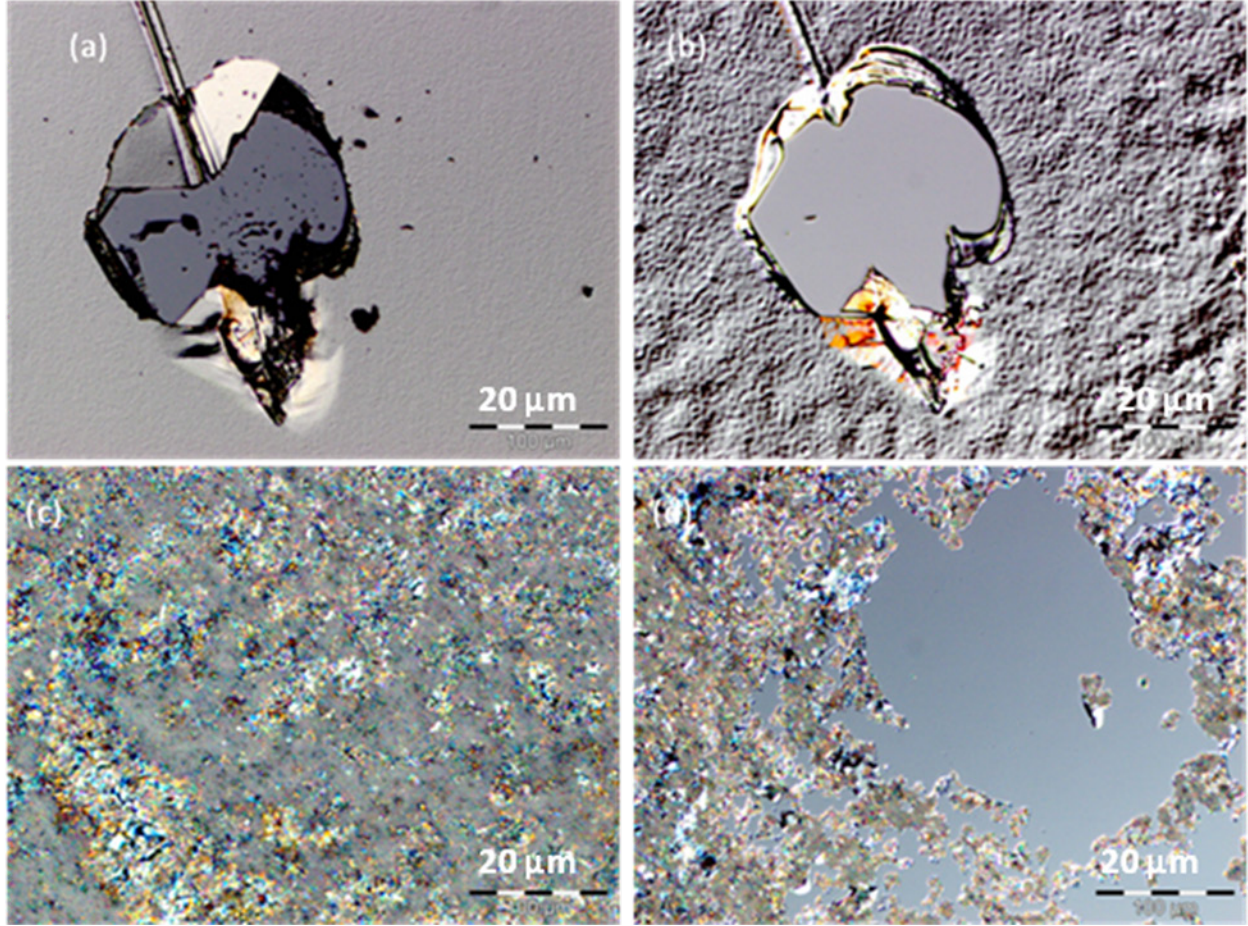


Fig. 11 Piece of ZT072406N viewed under Nomarski 20 \times a) unetched, and etched $\text{HNO}_3\text{:HCl:C}_3\text{H}_6\text{O}_3$ (2:1:2), b) 5 s, c) 10 s (center), and d) 10 s (near edge)

Given this effect, the etch rate for EPD measurements for these samples needs to be precisely controlled to ensure the etch solution does not reach the ZnTe buffer layer.

5. Further Work

While we now have etch solutions that can produce pits that could correspond to dislocations, further work is required to produce a standard EPD process for $\text{Hg}_{1-x}\text{Cd}_x\text{Se}$. The final EPD solution for $\text{Hg}_{1-x}\text{Cd}_x\text{Se}$ should have the following features:

1. **Consistent etch rate:** While some decrease in etch rate is to be expected as the solution sits out in the hood, that decrease needs to be slow enough for the etch to be consistent from sample to sample (unlike the solutions with phosphoric acid).
2. **Uniform across sample:** The pits appeared to be slightly different across the sample, suggesting the etch rate was not consistent across the surface. It was already noted that the

tweezers formed a partial etch-mask where they gripped the sample, so a slower motion was adopted when etching.

3. **Smaller pit size:** The $\text{HNO}_3\text{:HCl}$ (2:1) solution had the pits growing at a rate of $\sim 0.82 \mu\text{m/s}$. The rate at which the size of the pit grows needs to be slowed to minimize the pits overlapping.
4. **Slower etch rate:** The rate for the sample overall needs to be slowed so that the EPD versus depth can be more precisely measured.

In addition to developing an EPD solution with the characteristics listed above, polishing etch solutions for $\text{Hg}_{1-x}\text{Cd}_x\text{Se}$ will also be investigated. Through the course of this work, a better understanding of the etching kinetics of $\text{Hg}_{1-x}\text{Cd}_x\text{Se}$ will be obtained in order to develop better etching solutions.

6. References

1. Brill G, Chen Y, Wijewarnasuriya P. J. Elect. Mater. 2011;40:1679.
2. Wehyer JL, Kelly JJ. in Handbook of Crystal Growth. Berlin, Springer-Berlin Heidelberg, 2012, pp. 1453–1476.
3. Benson JD, Bubulac LO, Smith PJ, Jacobs RN, Markunas JK, Jaime-Vasquez M, Almeida LA, Stoltz AJ, Wijewarnasuriya PS, Brill G, Chen Y, Lee U, Vilela MF, Peterson J, Johnson SM, Lofgreen DD, Rhiger D, Patten EA, Goetz PM. J. Elect. Mater. 2010;39:1080.
4. Everson WJ, Ard CK, Sepich JL, Dean BE, Neugebauer GT, Schaake HF. J. Elect. Mater. 1995;24:505.
5. Doyle K, Swartz CH, Dinan JH, Myers TH, Brill G, Chen Y, VanMil BL, Wijewarnasuriya P. J. Vac. Sci. Technol. B 2013;31:03C124.
6. Walker P, Tarn WH. in CRC Handbook of Metal Etchants; Boca Raton, FL, CRC Press LLC, 1991, pp. 221 and 809.
7. Cobb SD, Szofran FR, Jones KS, Lehoczy SL. J. Elect. Mater. 1999;28:732.

List of Symbols, Abbreviations, and Acronyms

Br_2	bromine
$\text{C}_3\text{H}_6\text{O}_3$	lactic acid
CdSe	cadmium selenide
CH_3COOH	acetic acid
CH_3OH	methanol
EPD	etch pit density
GaSb	gallium antimonide
H_2O	water
H_2SO_4	sulfuric acid
H_3PO_4	phosphoric acid
HCl	hydrochloric acid
HF	hydrofluoric acid
$\text{Hg}_{1-x}\text{Cd}_x\text{Se}$	mercury cadmium selenide
$\text{Hg}_{1-x}\text{Cd}_x\text{Te}$	mercury cadmium telluride
HgSe	mercury selenide
HNO_3	nitric acid
IR	infrared
SEM	scanning electron microscopy
TEM	tunneling electron microscopy
ZnTe	zinc telluride

1 DEFENSE TECHNICAL
(PDF) INFORMATION CTR
DTIC OCA

2 DIRECTOR
(PDF) US ARMY RESEARCH LAB
RDRL CIO LL
IMAL HRA MAIL & RECORDS MGMT

1 GOVT PRINTG OFC
(PDF) A MALHOTRA

2 DIRECTOR
(PDF) US ARMY RESEARCH LAB
RDRL SEE I
KEVIN DOYLE
SUDHIR TRIVEDI

INTENTIONALLY LEFT BLANK.